4. With the passage of a pressure pulse through an interface between two media in the case when the wave resistance (ρc) of the second medium is lower (lower boundary of the packet, free surface), the reflected compression wave changes sign but the velocity remains the same. In the case when the wave resistance of the second medium is greater (upper boundary of the packet, well bottom, mouth of the central tube), the reflected compression wave retains its sign and the velocity changes to the opposite value.

5. The transmitted pressure pulse always retains the sign of the transmitted wave. Meanwhile, the amplitudes of the pressure pulses and the velocities of the incident, transmitted, and reflected (from the interface) waves are such as to satisfy the condition of equality of the total pressures and the normal components of velocity at the boundary.

NOTATION

$P(z, t)$, pressure in the channel; $q(z, t)$, volumetric flow rate of liquid; ρ, density of liquid; c, velocity of dynamic disturbances in the fluid; τ, shear stress; $\delta = f/\ell$, corrected hydraulic radius of pipe; f, cross section of channel; ℓ, perimeter of channel; α, gas content; ρ_g, ρ_ℓ, density of gas and liquid; c_g, c_ℓ, speed of sound in the gas and liquid; ρ_{g0}, density of gas under atmospheric conditions (at $P = P_{atm}$); K, N, constants in the exponential rheological model of the liquid; K_{ref}, reflection coefficient; L, length of channel; X, distance from the bottom to the lower boundary of the paket; D, D_2, inside and outside diameters of pipe; D_1, inside diameter of external pipe of the annular channel; H_{gp}, height of the gasified packet.

LITERATURE CITED

1. G. D. Rozenberg and I. V. Magdalinskaya, Dokl. Akad. Nauk SSSR, 255, No. 4, 625-627 (1980).
2. I. A. Charnyi, Nonsteady Motion of an Actual Liquid in Pipes [in Russian], Moscow (1975).
3. S. D. Tseitlin, Inzh. Fiz. Zh., 40, No. 4, 664-672 (1981).
4. A. M. Yasashin and R. V. Avetov, Neft. Khoz., No. 11, 24-27 (1980).
5. G. Wallace, One-Dimensional Two-Phase Flows [Russian translation], Moscow (1972).
6. L. M. Brekhovskikh and V. V. Goncharov, Introduction to Continuum Mechanics [in Russian], Moscow (1982).

NUMERICAL INVESTIGATION OF NONEQUILIBRIUM TWO-PHASE FLOWS IN AXISYMMETRIC LAVAL NOZZLES

P. M. Kolesnikov and V. V. Leskovets

UDC 533.6.011.3

A computation algorithm is elucidated and results are presented of the numerical solution of two-phase flow equations. A comparison is made with the experimental and computed data of other authors.

Flows of two-phase mixtures consisting of a gas and particles or drops suspended therein are extensively widespread in both nature and in technical applications. A set of typical examples of such two-phase flows can be presented. Certain of the natural phenomena are the motion of raindrops or snow in clouds and mist, dust and sand storms, scattering of particles of different origin in the atmosphere, etc. A broad circle of applied problems is associated with the flow and application of aerosols of different kinds, intensification of the heat and mass transfer processes in chemical production, natural gas transport, thermal and mechanical treatment of friable materials, etc.

Aviation and cosmonautics also inevitably encounter the solution of theoretical problems and the performance of extensive testing investigations in this area. Great value is attrib-

A. B. Lykov Institute of Mass and Heat Transfer, Academy of Sciences of the Belorussian SSR, Minsk.

Translated from Inzhenerno-Fizicheskii Zhurnal, Vol. 8, No. 1, pp. 27-35, January, 1990. Original article submitted September 26, 1988.

0022-0841/90/5801-0020$12.50

uted, in particular, to the investigation of flows in nozzles. Determination of the local stream parameters and the specific impulse with particle lag in velocity and temperature taken into account during mixture expansion in the nozzle was the main direction of the first researches [1-2].

At this time researches are known, [3-5], say, where regularities of two-phase heterogeneous stream motion are investigated in a more complex formulation in both the change in the stream components and in the nozzle configuration. Within the framework of a two-fluid (two-velocity and two-temperature) model of a continuous medium, solutions are obtained in this paper by using the build-up method and the Marsh method, that describe inviscid ideal gas flows without particles and flows of a gas mixture with foreign particles in the subsonic, transonic, and supersonic parts of a Laval nozzle. Solution of the problem in a two-dimensional formulation permits determination of the most important quantitative and qualitative characteristics of two-phase flows in nozzles: the site of particle incidence on the wall and their quantity, the location of the particle limit lines (particle-free zones), losses by dissipation, losses because of particle collision with the walls, and other inhomogeneous effects.

The problem under consideration, which is important to many applications, includes a number of other situations, whose analysis and utilization are often necessary even in other cases for the solution of problems within the framework of an analogous model of a continuous medium. The study of problems of such type occurred initially in researches of Kh. A. Rakhmatulin [6], R. I. Nigmatulin [7, 8], A. N. Kraiko [7, 9], L. E. Sternin [3, 7, 9] as well as in investigations of other authors [10-13].

1. FORMULATION OF THE PROBLEM

In addition to the assumptions made, as mentioned in [4], say, it is considered that the medium is two-fluid (two-velocity and two-temperature) [1, 10]. The real gas flow with particles therein is replaced by mutually-penetrating motion of the phases whose mass is distributed continuously over the whole volume. There are here two velocities and two temperatures at each point of the flow and the ratio between the mass of particles in a certain sufficiently small volume and its magnitude is understood to be the particle phase density (particle "gas") in conformity with the hypothesis of mutually penetrating continua [6]. It is also assumed that the distances in which the flow characteristics change substantially outside the surfaces of discontinuously are much greater than the spacings between particles, the Mach number of the relative particle motion is here less than critical while the viscosity and heat conductivity are taken into account only during gas and particle interaction processes.

A cylindrical x, y, φ, coordinate system whose OX axis agreed with the nozzle longitudinal axis (Fig. 1a) was used as initial coordinate system. The radial velocity component is denoted by v and the velocity component along the OX axis by u, where this latter is assumed always possible. It is convenient to realize the two-dimensional flow computations on meshes connected with the surface of the computation domain which requires a coordinate transformation. In this case the flow domain was rectified by replacement of the independent variables $\xi = y/Y(x)$ or $\eta = y/Y_S(x)$.

Initial Equations. The initial inviscid gas equations (continuity, momentum, energy) for an axisymmetric two-phase stationary flow are written in the following form [7, 13]

$$\nabla y\rho \mathbf{U} = 0,\ \nabla y\rho u\mathbf{U} + (yp)_x = yC_R\rho_s(u_s - u),\ \nabla y\rho v\mathbf{U} + (yp)_y - p = \tag{1}$$

$$= yC_R\rho(v_s - v),\ \nabla y\rho H_0\mathbf{U} = y\rho_s\{C_\alpha(T_s - T) + C_R[u_s(u_s - u) + v_s(v_s - v)]\};$$

$$\nabla y\rho_s\mathbf{U}_s = 0,\ \nabla y\rho_s u_s\mathbf{U}_s = y\rho_s C_R(u - u_s),\ \nabla y\rho_s v_s\mathbf{U}_s = y\rho_s C_R(v - v_s),$$

$$\nabla y\rho_s T_s\mathbf{U}_s = y\rho_s C_\alpha\frac{c_p}{c_B}(T - T_s). \tag{2}$$

The equation of state and dependences for the coefficients C_R and C_α are needed to close the system of equations. For the ideal gas model taken in this paper with a constant adiabatic index, the equation of state is written in the form

$$p = \rho\frac{k-1}{k}[H_0 - (u^2 + v^2)/2]. \tag{3}$$

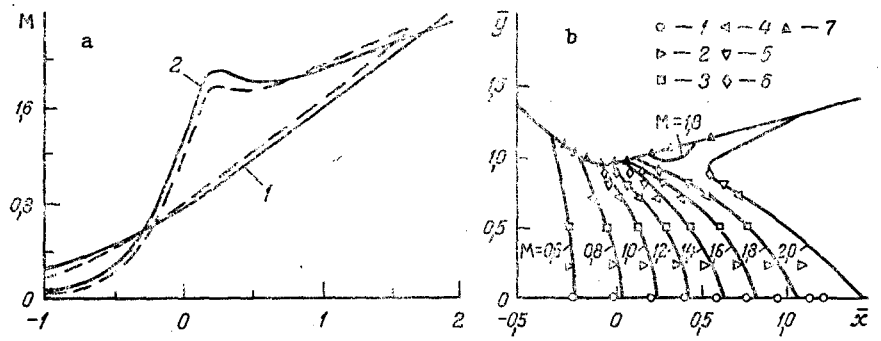

Fig. 1. Comparison of computation results on the Mach number distribution (solid lines): a) with data of a numerical solution [5] (dashed lines: r_s = 10 μm, z = 0.3; the numbers on the computed curves correspond to: 1) axis; 2) wall of the nozzle); b) with experiment [19] (1) axis; 2) $\bar{y}$ = 0.25; 3) 0.519; 4) 0.738; 5) 0.837; 6) 0.913; 7) wall).

The depence obtained in [14] was used for the coefficient C_R for the subsonic, transoinc, and supersonic flow modes.

The expression from [2] with the Cavanaugh correction [15] taken into account for the influence of gas inertia and rarefaction:

$$C_\alpha = C_{\alpha 0}\,\mathrm{Nu}_0/[1 + 3{,}42M\mathrm{Nu}_0/(\mathrm{RePr})],$$

$$\mathrm{Nu}_0 = 2 + 0{,}459\mathrm{Re}^{0{,}55}\mathrm{Pr}^{0{,}33},\quad C_{\alpha 0} = 1{,}5\mu/(\rho_B r^2 \mathrm{Pr})$$

was used for the heat elimination coefficient C_α. The temperature dependence of the molecular viscosity is set up by using the power law

$$\mu/\mu_0 = (T/T_0)^{0{,}71}.$$

The change in ρ_s for Al_2O_3 as a function of the temperature is [16]

$$\rho_s = 3{,}06 - 0{,}967\cdot 10^{-3}(T_s - 2323)\ [\mathrm{g/cm^3}].$$

The initial system of equations consists of two subsystems (1), (3), and (2) describing the gas and particle flow. The first subsystem is of elliptic-hyperbolic type in the sub- and transonic parts of the Laval nozzle and is hyperbolic in the supersonic part. The system (2) is of hyperbolic type for $u_s > 0$ which is ordinarily satisfied in nozzles.

Boundary and Initial Conditions. The flow in the nozzle was separated into two subdomains. The first, the sub- and transonic subdomain, is bounded on the left by the nozzle entrance section $x = x_0$, on the right by the line $x = x_1$ at which the Mach number determined from the "frozen" speed of sound equals

$$M_x = u(x_1, y)/a(x_1, y).$$

The second is the supersonic domain bounded on the left by $x = x_1$ and on the right $x = x_c$.

Conditions for a completely frozen flow are given at the nozzle entrance. The flow is here assumed equilibrium and three boundary conditions [11] were given for the nonstationary analog of (1):

1) Constancy of the total enthalpy

$$H_0 = \frac{k}{k-1}\frac{p}{\rho} + \frac{1}{2}(u^2 + v^2) = \mathrm{const};$$

2) Constancy of the entropy

$$S = p/\rho^k = \mathrm{const};$$

3) The velocity vector direction

$$v/u = \xi \cdot \frac{d}{dx} Y(x)\Big|_{x=x_0}.$$

The particle parameters (except the density) at the entrance were assumed equal to the corresponding gas parameters

$$\rho_s(x_0, y) = \frac{z}{1-z}\rho(x_0, y).$$

The condition of nonpenetration

$$v[x, Y(x)]/u[x, Y(x)] = \frac{d}{dx}Y(x)$$

was given on the nozzle wall. The standoff of particle trajectories from the wall corresponds to the appearance of the upper boundaries of the particles (the particle limit line), whose position is determined by the solution of the system (2).

Flow symmetry conditions were given on the nozzle axis

$$v = 0, \ (u)_y = (\rho)_y = (p)_y = 0.$$

The initial data for analysis of the supersonic domain were selected after computation of the first sub- and transonic domains on the coordinate line $x = x_2$ near the minimal nozzle section on which the Mach number is $M \geq 1.01$ on the nozzle axis. To eliminate the influence of gas parameter interpolation on the right boundary during computation of the first domain on the flow parameters in the supersonic domain it was assumed $x_2 < x_1$, i.e., the computed domains were made to overlap.

2. METHOD OF SOLUTION

Solution of Sub- and Transonic Flow Problems. Solutions were sought successively in the first (sub- and transonic) and second (supersonic) domains, where step-by-step (Marsh) integration of (1), (3) and (2) along the longitudinal coordinate is most effective for purely supersonic flows. The stationary solutions in the sub- and transonic domain are obtained by the build-up method [11], i.e., by integration of nonstationary equations in time for stationary boundary conditions until changes in the solution become sufficiently small. In this case just the system (1), which is of mixed type in this domain (sub- and transonic), was replaced by the nonstationary system since the system (2) is of hyperbolic type even in the subsonic part by virtue of the condition $u(x, y) > 0$. The flow computation is realized as follows. The stationary system (2) is integrated for known gas parameter fields before the beginning of the calculation of the new step in time and the right sides for the system (1) are computed and stored also. Then the stationary solution of the system (1) is found in the new time layer by the build-up method for fixed values of the right sides, and the procedure is later repeated.

A finite-difference method was used for numerical integration of the system (1). The explicit conservative MacCormack scheme [17] of second order accuracy was used for the difference approximation of the equations.

Solution of the Problem of Supersonic Stationary Two-phase Flow in Laval Nozzles. A two-step explicit-implicit scheme of the predictor-corrector type, also of second order accuracy [13], but without the constraints on the integration step because of the quantities C_R, C_α governing the "hardness" of the system, were used to integrate the system (2) in the "hard" class.

Let us represent the system (2) vectorally in new independent variables

$$(\mathbf{A})_x + (\mathbf{B})_\eta + \mathbf{C}(\mathbf{A} - \mathbf{D}) = 0, \tag{4}$$

$$\mathbf{A} = \begin{bmatrix} 1 \\ u_s \\ v_s \\ T_s \end{bmatrix} \eta Y_s^2 \rho_s u_s, \quad \mathbf{B} = \eta Y_s (v_s - \eta Y_{sx} u_s) \begin{bmatrix} \rho_s \\ \rho_s u_s \\ \rho_s v_s \\ \rho_s T_s \end{bmatrix};$$

$$\mathbf{C} = \begin{bmatrix} 0 & 0 & 0 & 0 \\ 0 & C_R/u_s & 0 & 0 \\ 0 & 0 & C_R/u_s & 0 \\ 0 & 0 & 0 & (C_\alpha/u_s)(c_p/c_B) \end{bmatrix}, \quad \mathbf{D} = \eta Y_s^2 \rho_s u_s \begin{bmatrix} 0 \\ u \\ v \\ T \end{bmatrix},$$

$$Y_{sx} = \frac{d}{dx} Y_s(x).$$

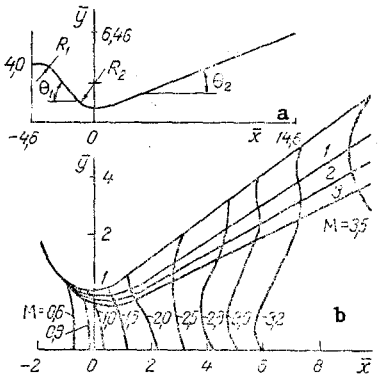

Fig. 2. Mach number isoline distribution and location of limit lines of particles of different radii (1) 0.5 μm; 2) 3.0; 3) 8.5) for z = 0.32 (b) in the axisymmeric nozzle (a).

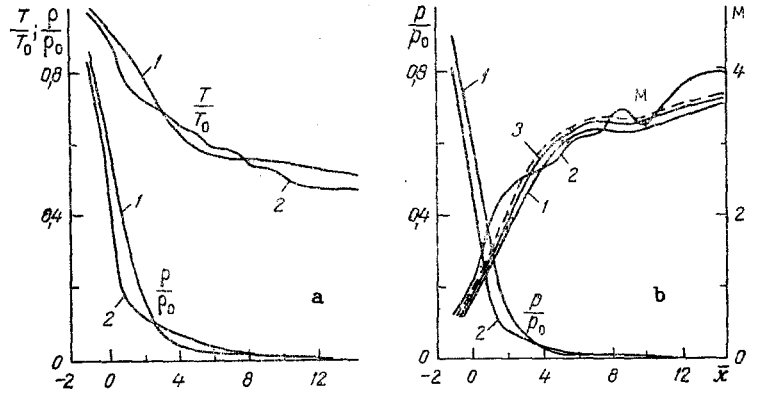

Fig. 3. Change of parameters on the axis and wall (T/T_0, ρ/ρ_0, p/p_0, M) along the nozzle length (notation the same as in Fig. 1a), the dashes and line 3 are, respectively, the Mach number profile on the axis for a gas without particles and for a stream with r_s = 1 μm.

The difference scheme is written in the predictor stage as

$$(\hat{\mathbf{A}}_j^{n+1} - \mathbf{A}_j^n)/\Delta x + (\mathbf{B}_{j+1}^n - \mathbf{B}_j^n)/\Delta\eta + \mathbf{C}^n(\hat{\mathbf{A}}_j^{n+1} - \hat{\mathbf{D}}_j^{n+1}) = 0, \tag{5}$$

where the components of the vector $\hat{\mathbf{D}}_j^{n+1}$ are obtained from the first step of the MacCormack scheme during integration of the equations of the system (1) while $Y_s^2\rho_s u_s$ are obtained from (5) for the first component of the vector A, since the corresponding components of the vectors **C** and **D** are zero here.

The corrector step is

$$(\mathbf{A}_j^{n+1} - \mathbf{A}_j^n)/\Delta x + [(\hat{\mathbf{B}}_j^{n+1} - \hat{\mathbf{B}}_{j-1}^{n+1}) + (\mathbf{B}_{j+1}^n - \mathbf{B}_j^n)]\frac{1}{2\Delta\eta} +$$

$$+ \mathbf{C}_j^{n+1/2}(\mathbf{A}_j^{n+1/2} - \mathbf{D}_j^{n+1/2}) = 0,$$

$$\mathbf{C}_j^{n+1/2} = (\hat{\mathbf{C}}_j^{n+1} + \mathbf{C}_j^n)/2,\ \mathbf{D}_j^{n+1/2} = (\mathbf{D}_j^{n+1} - \mathbf{D}_j^n)/2. \tag{6}$$

The term $\mathbf{A}_j^{n+1/2}$ is obtained from the Taylor series expansion

$$\mathbf{A}_j^{n+1/2} = \mathbf{A}_j^{n+1} - \frac{\Delta x}{2}(\partial\mathbf{A}/\partial x)_j^{n+1}.$$

The derivative $(\partial\mathbf{A}/\partial x)_j^{n+1}$ is determined from [11]. After a number of manipulations, we finally obtain

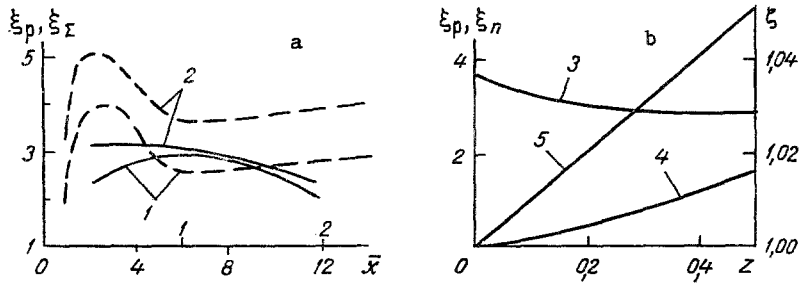

Fig. 4. Change in the loss of specific impulse: a) by dissipation ξ_p (curve 1) and total losses ξ_Σ (2) for the nozzle [1] (see Fig. 2a) for z = 0.32 (dashed lines) and the nozzle from [5] for z = 0.3 (solid lines): b) by dissipation (curve 3) and the two-phase state (4) at the exit of the first nozzle and change in the mass flow rate coefficient (5) for different z.

$$\hat{\mathbf{A}}_j^{n+1} = \frac{\mathbf{A}_j^n - \frac{\Delta x}{\Delta \eta}(\mathbf{B}_{j+1}^n - \mathbf{B}_j^n) + \Delta x \mathbf{C}_j^n \hat{\mathbf{D}}_j^{n+1}}{1 + \Delta x \mathbf{C}_j^n}, \tag{7}$$

$$\mathbf{A}_j^{n+1} = \left[\mathbf{A}_j^n + (1 + \Delta x \mathbf{C}_j^n)\hat{\mathbf{A}}_j^{n+1} - (1 + \Delta x \hat{\mathbf{C}}_j^{n+1/2}) \frac{\Delta x}{\Delta \eta}(\hat{\mathbf{B}}_j^{n+1} - \hat{\mathbf{B}}_{j-1}^{n+1}) + \right.$$

$$\left. + 2\Delta x \left(\frac{\Delta x}{2} \hat{\mathbf{C}}_j^{n+1} \hat{\mathbf{D}}_j^{n+1} + \hat{\mathbf{D}}_j^{n+1/2} \right) \mathbf{C}_j^{n+1/2} - \Delta x \mathbf{C}_j^n \mathbf{D}_j^{n+1} \right] \times$$

$$\times \left[2 + \Delta x \mathbf{C}_j^{n+1/2} + \frac{(\Delta x)^2}{2} \hat{\mathbf{C}}_j^{n+1} \mathbf{C}_j^{n+1/2} \right]^{-1}.$$

The components of the vector $\mathbf{D}_j^{n+1}$ are obtained by the same algorithm as for $\hat{\mathbf{D}}_j^{n+1}$ in the corrector step. Analysis of the stability of the scheme (5) and (8) results in a Courant type condition [18]

$$\Delta x \leqslant \Delta \eta Y_s / (v_s / u_s - \eta Y_{sx}).$$

The constraint obtained on the integration step does not result in a noticeable increase in the computation time, as computations showed.

Utilization of the build-up method requires preliminary assignment of the condition for achieving convergence. The selection of such a condition is made on the basis of studying the nature of the change in the magnitude of a single nozzle pulse during the trial computations. Damped vibrations of this quantity were observed in all cases. The flow is considered steady if the magnitude of the single nozzle pulse changed by not more than 0.01% in a time interval of 100 steps.

3. RESULTS OF COMPUTATIONS

Flow in an axisymmetric supersonic nozzle with a small radius of throat curvature R_2 = 0.625 was computed to determine the possibilities and verify the numerical method [5, 19]. The nozzle conical sections were mated smoothly with the arcs of circles; the slope of the conical subsonic section was 45°, and of the conical supersonic section 15°. Results of the computations were compared with results obtained in [5] by a numerical method using a MacCormack difference scheme and with experimental data without taking account of the two-phase state [19]. The initial data in both comparisons were taken equal to the corresponding parameters in [5, 19]. Results of the computations on the Mach number distribution along the nozzle length on the axis and wall (curves 1 and 2, respectively) are presented in Fig. 1a, where the results obtained are displayed by solid lines while the data of [5] are dashed. The Mach number isoline distribution in the neighborhood of the nozzle critical section is shown in Fig. 1b, where the parameter gradients are largest. The experimental data of [19] are denoted by geometric figures for different radii y while the curves display the Mach number isolines obtained by using the numerical method of this paper. Results of the proposed method are compared with data from [5] in a broad range of radii and weight fractions of particles (r_s = 10 μm, z = 0.3 in Fig. 1a). On the whole the agreement between the results of the numerical solution and the data in [5] can be considered completely satisfac-

tory. Agreement between the computed and experimental data along the nozzle radius is good enough up to the value $\bar{x} < 1.0$, but there are differences here in the neighborhood of the nozzle axis (Fig. 1b). It is quite important to know the magnitude of the gasdynamic losses of specific impulse and the nature of the loss change along the nozzle channel for a computation of the nozzle characteristics of real engineering apparatus. The specific impulse loss distribution due to dissipation and the total losses (solid lines) obtained as the difference between the equilibrium and real specific impulse of a two-dimensional two-phase flow is presented in Fig. 4a for the nozzle under consideration.

The two-phase flow configuration was computed in nozzles of different geometry. An axisymmetric conical nozzle with a large magnitude of the throat radius of curvature (R_2 = 2.01) is shown in Fig. 2a. Its contour consists of the sections:

1) Cylindrical entrance part ($-4.6 \leq \bar{x} \leq -3.9$), $\bar{y} = 4$; here and below all the dimensions are referred to the radius of the nozzle minimal section r*;

2) Arcs of a circle of radius $R_1 = 1.15$ ($-3.9 \leq x \leq -2.94$);

3) Cone with half-angle $\theta_1 = 52°$ ($-2.94 \leq \bar{x} \leq 1.65$);

4) Arcs of a circle wtih radius $R_2 = 2.01$ with center on the $\bar{y}$ axis ($-1.65 \leq \bar{x} \leq 0.74$);

5) Cone with half-angle $\theta_2 = 20°$ ($0.74 \leq \bar{x} \leq 14.6$).

The coordinates of the entrance section are $\bar{x}_c = 15.6$, $\bar{y}_c = 6.46$. All the line segments and arcs of circles are mated smoothly and the computations were performed for nozzles with different critical section radius.

This nozzle contour was approximated in a table by using polynomial interpolation [20], and the possibility was provided here for both a single approximation of the whole nozzle contour and independently in each of the sections.

The following initial data were taken at the nozzle entrance for a model combustion products composition [2, 3]: k = 1.14, p_0 = 9 MPa, T_0 = 3100 K, ρ_0 = 8.234 kg/m^3, m = 26.2 kg/kmole, $\mu_0 = 8.937 \cdot 10^{-5}$ kg/(m·C), Pr = 0.69, C_B = 1876 J/(kg·K), r_s = 10 μm, and z = 0.32.

Computations were performed for nozzles with the critical section radius 0.01 m, the dimensions and mass fraction of the particles were varied within sufficiently broad limits (r_s = 0.5-10 μm, z = 0.1-0.5).

The Mach number isoline distribution and limit lines of particles of different radii are represented in Fig. 2b for a constant weight fraction of condensate z = 0.32. The comparison of the flow parameters on the axis and the wall of the nozzle along the longitudinal coordiante (notation the same as in Fig. 1a) is displayed in Fig. 3 for a model combustion product composition. The parameters are given in dimensionless form, which is achieved by referring them to the corresponding frozen parameters at the nozzle entrance: the pressure to p_0, the temperature to T_0, the density to ρ_0. Mach number profiles on the axis are presented here for a gas without particles (dashed lines) and for a two-phase flow with particles of 1 μm radius for an invariant z equal to 0.32 (Fig. 3b). It is seen that as the particle size increases the Mach number profiles for the two-phase flow and the gas without particles do not change substantially. This is explained by the diminution in the total particle area resulting in a reduction in the energy and momentum transfer between the gas and the particles. The same occurs also for a diminution in the weight fraction of condensate particles.

Results of computations of a number of two-phase flow integral characteristics are presented in Fig. 4. The change in the loss of specific impulse by dissipation and the total losses along the nozzle channel is shown in Fig. 4a (dashed lines). Values of the loss by dissipation and the two-phase state as the change in the mass flow rate factor ζ at the nozzle exit are determined for different z (fig. 4b). The magnitude of the two-phase losses was calculated as the difference between single impulses of equilibrium and nonequilibrium two-phase axisymmetric flows. The integral characteristics represented, as well as the results of computations performed to determine the specific impulse loss for different radii of the nozzle critical section are in good agreement with the results of existing computations [2, 13].

In conclusion, the authors are grateful to A. D. Rychkov for assistance in problem and program formulation.

NOTATION

$\mathbf{U} = u\mathbf{i} + v\mathbf{j}$, velocity vector; $\mathbf{i}$, $\mathbf{j}$, unit vectors of the basic x, y, φ cylindrical coordinate system; ρ, density; p, pressure; T, temperature; C_R, C_α are the drag and heat transfer coefficients, respectively; H_0, stagnation enthalpy; c_p/c_B, ratio between the specific heats of the gas at constant pressure and the particle material; k, gas adiabatic index ("frozen"); $M=|\mathbf{U}-\mathbf{U}_s|/a$, Mach number; a, speed of sound; $\mathrm{Re} = 2r\rho|\mathbf{U}-\mathbf{U}_s|/\mu$, gas flow Reynolds number moving relative to the particle of radius r_s; μ, gas viscosity coefficient; S, gas entropy; z, weight fraction of particles; Y(x), nozzle contour; $Y_s(x)$, particle limit line; ξ, η, transformed curvilinear coordinates; x, y, coordinates referred to the nozzle critical section radius r_*; **A**, **B**, **C**, **D** vector quantities in (4); m, the mixture molecular mass, and Pr, Prandtl number.

Subscripts: $()_x$, partial derivative with respect to x; $()_y$, partial derivative with respect to y; s, B, values referring to the parameters and the particle material; 0 is the value of the parameter at the stagnation point; and n, j, integers.

LITERATURE CITED

1. J. Kliegel and H. Nickerson, Detonation and Two Phase Flow, P. F. Pokhil (ed.) [Russian translation, 183-201, Moscow (1966).
2. V. E. Alemasov, A. F. Dregalin, A. P. Tishin, and V. A. Khudyakov, Thermodynamical and Thermophysical Properties of Combustion Products [in Russian], Vol. 1, 190-213 (1971).
3. L. E. Sternin, Principles of the Gasdynamics of Two-phase Flow in Nozzles [in Russian], Moscow (1976).
4. A. D. Rychkov and A. A. Schraiber, Izv. Akad. Nauk SSSR, Mekhan. Zhidk. Gaza, No. 3, 73-79 (1985).
5. Cheng Ishi, AIAA J., No. 12, 59-67 (1980).
6. Kh. A. Rakhmatulin, Prikl. Matem. Mekhan., 20, No. 2, 184-195 (1986).
7. A. N. Kraiko, R. I. Nigmatulin, V. K. Starkov, and L. E. Sternin, Science and Engineering Surveys. Hydromechanics [in Russian], 6, 127-153, Moscow (1972).
8. R. I. Nigmatulin, Principles of Mechanics of Heterogeneous Media [in Russian], Moscow (1978).
9. A. N. Kraiko and L. E. Sternin, Prikl. Matem. Mekhan., 29, 415-429 (1965).
10. P. M. Kolesnikov and A. A. Karpov, Nonstationary Two-phase Gas-liquid Flows in Channels, R. I. Soloukhin (ed.) [in Russian], Minsk (1986).
11. I. M. Vasenin and A. D. Rychkov, Izv. Akad. Nauk SSSR, Mekhan. Zhidk. Gaza, No. 5, 178-181 (1973).
12. V. I. Kopchenov and A. N. Kraiko, Scient. Trans., Moscow Univ. Mechanics Institute [in Russian], No. 23, 96-108 (1974).
13. A. A. Glazunov and A. D. Rychkov, Izv. Akad. Nauk SSSR, Mekhan. Zhidk. Gaza, No. 6, 86-91 (1977).
14. Henderson, AIAA J., No. 6, 5-7 (1976).
15. D. Carlson and R. Hoaglund, AIAA J., No. 1, 104-109 (1964).
16. É. É. Shpil'rain and K. A. Yakimovich, "Thermphysical Properties of Beryllium Oxide and Aluminum Oxide in the 1000-3700 K Temperature Range (Generalized Handbook Dat) [in Russian], Report Inst. Vysok. Temp. Akad. Nauk SSSR (1974).
17. R. W. MacCormack, AIAA Paper No. 354 (1969).
18. V. F. Nokh, Computational Methods in Hydrodynamics [in Russian], Moscow (1967).
19. Kaffel, Beck and Massey, AIAA J., No. 7, 184-187 (1969).
20. A. A. Blynskaya, Yu. B. Lifshits, and V. D. Perminov, Uch. Zap., TsAGI, 5, No. 1 (1974).